Two Anhydrous Zeolite X Crystal Structures, $Mn_{28}Cs_{36}$-X and $Mn_{21.5}Rb_{49}$-X

Myung Nam Bae,† Mee Kyung Song, and Yang Kim*

Department of Chemistry and Chemistry Institute for Functional Materials, Pusan National University, Pusan 609-735, Korea
Received June 7, 2001

The crystal structures of fully dehydrated Mn^{2+}- and Cs^+-exchanged zeolite X, $Mn_{28}Cs_{36}$-X (X=$Si_{100}Al_{92}O_{384}$; a = 24.732(1) Å), and Mn^{2+}- and Rb^+-exchanged zeolite X, $Mn_{21.5}Rb_{49}$-X (a = 24.742(1) Å), have been determined by single-crystal X-ray diffraction methods in the cubic space groups $Fd\bar{3}m$ and $Fd\bar{3}$ at 21(1) °C, respectively. Two crystal structures were refined to the final error indices R_1 = 0.069 and R_2 = 0.054, with 130 reflections, and R_1 = 0.087 and R_2 = 0.071, with 203 reflections, respectively, for which $I > 3\sigma(I)$. In $Mn_{28}Cs_{36}$-X, 28 Mn^{2+} ions per unit cell were found at three crystallographic sites: 14 at site I, 4 at site I′, and the remaining 10 at site II. The Mn^{2+} ion at site II was recessed 0.47(1) Å into the supercage, where it was coordinated to three framework oxygens at 2.16(1) Å. Thirty-six Cs^+ ions were found at three sites: 7 at site II′, 7 at site II, and 22 at site III. The Cs^+ ion at site II was recessed 2.16(1) Å into the supercage, where it was coordinated to three framework oxygens at 2.93(1) Å. Most of the Mn^{2+} ions at site I were not exchanged with Cs^+ ions but some Mn^{2+} ions at site II were disturbed and exchanged with Cs^+ ions. In $Mn_{21.5}Rb_{49}$-X, 21.5 Mn^{2+} ions were found at three sites: 11.5 at site I, 6 at site II′, and 4 at site I′. Forty-nine Rb^+ ions were found at four sites: 5 at site I′, 18 at site II, 6 at site II′, and 20 at site III. The Rb^+ ion at site II was recessed 1.876(4) Å into the supercage, where it was coordinated to three framework oxygens at 2.71(2) Å. The Mn^{2+} ions at site I and II were disturbed and exchanged with Rb^+ ions. Rb^+ ions, which are smaller and more diffusible than Cs^+ ions, occupied site I′. The maximum Cs^+ and Rb^+ ion exchanges were 39% and 53%, respectively. Because these cations were too large to enter the small cavities and their charge distributions in the zeolite structure may have been unfavorable, cation-sieve effects were shown.

Keywords : Structure, Zeolite X, Manganese, Cesium, Rubidium.

Introduction

The catalytic importance of zeolite X has prompted numerous investigations into the physical and chemical nature of this crystalline aluminosilicate. The role played in catalysis by cations associated with the zeolite framework also has received considerable attention.[1,2] Thus, the positions of cations in the zeolite must be known to ascertain their role in catalytic reactions.

The cationic positions in dehydrated Na-X have been reported four times in recent years.[3-6] The distribution and coordination of various cations in the framework of faujasite-type zeolites have been widely studied[7-15] and reviewed.[16] The selectivity of cations varies with the degree of cation exchange. Because of their size, cations at site I in the hexagonal prisms are the most difficult to exchange for large cations, such as Rb^+ and Cs^+ ions. This is referred to as the cation-sieve effect, that is, the entering cations cannot reach all of the sites occupied by the ions initially in the zeolite. The maximum degree of Rb^+ or Cs^+ ion exchange has been reported to be 65-80%.[17-19] Zeolite structures have unique features that lead to unusual types of cation selectivity and sieving. The cation exchange in zeolites is accompanied by dramatic alterations in stability, adsorption behavior, selectivity, catalytic activity, and other physical properties. Because many of these properties depend on controlled cation exchanges with particular cation species, a detailed structural analysis of cation-exchanged zeolite is important.

In the structure of $Ca_{35}Cs_{22}$-X,[20] 35 Ca^{2+} ions occupy sites I and II, and 22 Cs^+ ions are found at sites II′, II, and III. In the structure of $Ca_{31}Rb_{30}$-X,[21] 31 Ca^{2+} ions occupy sites I and II, and 30 Rb^+ ions are found at sites II′, II, and III. The small and highly charged Ca^{2+} ions prefer to occupy site I, where they can balance the anionic charge of the zeolite framework, and the remainder of the Ca^{2+} ions go to site II. The large Cs^+ and Rb^+ ions fill site II with the remainder of them going to the least suitable cationic site III. In the fully dehydrated Mn_{46}-X,[8] 16 Mn^{2+} ions fill site I, and the remaining 30 are at site II. These Mn^{2+} ions at sites I and II also can be exchanged with the second entering cations. However, in many cases, the cation selectivity varies with the degree of exchange, and the cations show the cation-sieve effect.

The present study investigates the site selectivity and the cation-sieve effect of Mn^{2+}, Cs^+, and Rb^+ ions within the zeolite X and delves into the geometry of their structures. As mentioned above, the structural stability and the catalytic property of zeolites depend on the type and number of

†Present address: Division of Molecular & Life Science, Pohang University of Science and Technology, Kyungbuk 790-784, Korea
*To whom all the correspondance should be addressed. Fax: +82-51-516-7421, e-mail: ykim@hyowon.pusan.ac.kr

cations and their distribution over the available sites. Therefore, it is important to determine the cationic positions and occupancies in zeolite.

Experimental Section

Single crystals of synthetic sodium zeolite X, with the stoichiometry of $Na_{92}Al_{92}Si_{100}O_{384}$, were prepared in St. Petersburg, Russia.[22] Each of two single crystals, a colorless octahedron with a cross-section of about 0.2 mm, was lodged in a fine Pyrex capillary for ion exchange. $Mn_{28}Cs_{36}$-X and $Mn_{21.5}Rb_{49}$-X were prepared using an exchange solution of 0.05 M $Mn(NO_3)_2$ for three days and then using each solution of $CsNO_3$ and CsOH, and $RbNO_3$ and RbOH in the molar ratio of 1 : 1, with a total concentration of 0.05 M for five days. The solution was allowed to flow past the crystals at a velocity of approximately 15 mm/s. The crystals were dehydrated at 400 °C under 2×10^{-6} Torr for 2 days. After cooling to room temperature, each crystal, still under vacuum, was sealed in a Pyrex capillary with a torch.

Diffraction data were collected with an automated four-circle Enraf-Nonius CAD4 diffractometer equipped with a scintillation counter, a pulse height analyzer, and a VAX computer. Molybdenum K_α radiation ($K_{\alpha1}$, λ = 0.70930 Å; $K_{\alpha2}$, λ = 0.71359 Å) with a graphite monochromater was used for all experiments. The cubic unit cell constant, a, determined by a least-squares refinement of 25 intense reflections for which $14^o < 2\theta < 24^o$ at 21(1) °C were 24.732 (1) Å and 24.742(1) Å for $Mn_{28}Cs_{36}$-X and $Mn_{21.5}Rb_{49}$-X, respectively.

All unique reflections in the positive octant of an F-centered unit cell for which $2\theta < 50^o$, $l > h$, and $k > h$ were recorded. Of 1,344 reflections measured for $Mn_{28}Cs_{36}$-X and 1,348 reflections for $Mn_{21.5}Rb_{49}$-X, only 130 and 203 reflections, respectively, for which $I > 3\sigma(I)$, were used in the subsequent structure determination. Calculations were performed with the structure determination package programs, *MolEN*.[23]

Absorption corrections (for $Mn_{28}Cs_{36}$-X, μR = 0.339 and ρ_{calc} = 1.950 g/cm^3; for $Mn_{21.5}Rb_{49}$-X, μR = 0.479 and ρ_{calc} = 1.733 g/cm^3) were made empirically using a Ψ scan.[24] The calculated transmission coefficients ranged from 0.982 to 0.997 for $Mn_{28}Cs_{36}$-X, and from 0.730 to 0.943 for $Mn_{21.5}Rb_{49}$-X. These corrections had little effect on the final R indices. The summary of data collection and the crystal structure determination are presented in Table 1.

Structure Determination

$Mn_{28}Cs_{36}$-X. In this structure, the space group $Fd\bar{3}$ was chosen initially because most crystals made from this synthesized batch have been refined successfully in $Fd\bar{3}$, with the mean Al-O distances being longer than the mean Si-O distances.[7-15] However, $Fd\bar{3}$ was later rejected and $Fd\bar{3}m$ was chosen because (a) in the least-squares refinement with $Fd\bar{3}$, there was no difference between the mean Al-O and the Si-O distance - the long-range Si, Al ordering had been lost; and (b) this crystal has intensity symmetry across (110) and therefore has this mirror plane. The diffraction data refined to almost the same error indices in $Fd\bar{3}m$.

A full-matrix least-squares refinement was initiated by using the atomic parameters of the framework atoms [Si, Al, O(1), O(2), O(3), and O(4)] in $Na_{60}H_{32}$-X.[25] The initial isotropic refinement of the framework atoms converged to an R_1 index, $(\Sigma \mid F_o - \mid F_c \mid \mid / \Sigma F_o)$, of 0.39 and a weighted R_2 index, $(\Sigma w(F_o - |F_c|)^2/\Sigma w F_o^2)^{1/2}$, of 0.36.

A difference Fourier function revealed four large peaks at (0.0, 0.0, 0.0), (0.162, 0.162, 0.162), (0.432, 0.125, 0.125), and (0.262, 0.262, 0.262), with heights of 7.3, 5.4, 4.7, and 4.2 eÅ^{-3}, respectively. These four positions were stable in the least-square refinement. The isotropic refinement that included these peaks as Mn(1), Cs(1), Cs(2), and Cs(3) converged to R_1 = 0.155 and R_2 = 0.135.

A subsequent difference Fourier function revealed two peaks: one at Mn(2) (0.224, 0.224, 0.224), with a height of 2.5 eÅ^{-3}, and another at Mn(3) (0.066, 0.066, 0.066), with a

Table 1. Crystallographic Data

	$Mn_{28}Cs_{36}$-X	$Mn_{21.5}Rb_{49}$-X
Space group	$Fd\bar{3}m$	$Fd\bar{3}$
Unit cell constant, a (Å)	24.732(1)	24.742(1)
ρ_{calcd} (g/cm^3)	1.950	1.733
Diffractometer	Enraf-Nonius CAD-4	Enraf-Nonius CAD-4
Data collection temperature (°C)	21	21
Radiation (Mo K_α) λ_1(Å)	0.70930	0.70930
λ_2(Å)	0.71359	0.71359
Number of reflections gathered	1344	1348
Number of observed reflections ($I > 3\sigma(I)$)	130	203
Number of parameters n_p	27	38
R indices ($I > 3\sigma(I)$)	R_1 [a]= 0.069, R_2 [b]= 0.054	R_1 = 0.087, R_2 = 0.071
R indices (all data)	R_1 = 0.208, R_2 = 0.061	R_1 = 0.296, R_2 = 0.109
Goodness-of-Fit [c]	1.27	2.06

[a]$R_1 = (\Sigma(F_o - \mid F_c \mid)/\Sigma F_o)$. [b]$R_2 = (\Sigma w(F_o - \mid F_c \mid)^2/\Sigma w F_o^2)^{1/2}$. [c]Goodness-of-Fit (error in an observation of unit weight) = $(\Sigma w(F_o - \mid F_c \mid)^2/(n - n_p))^{1/2}$ where n is the number of observed reflections and n_p is the number of parameters.

Table 2. Positional, Thermal, and Occupancy Parameters[a]
(a) Mn_{28} Cs_{36}-X

Atom	Wyc. Pos.	Site	*x*	*y*	*z*	U_{iso}[b]	Occupancy[c] Varied	Occupancy[c] Fixed
(Si, Al)	192(i)		–533(1)	1221(2)	358(2)	129(6)		192
O(1)	96(g)		–1080(3)	1080(3)	0	251(39)		96
O(2)	96(g)		–28(4)	–28(4)	1469(4)	356(37)		96
O(3)	96(g)		–634(3)	–634(3)	356(5)	253(37)		96
O(4)	96(g)		1688(3)	1688(3)	3154(5)	227(35)		96
Mn(1)	16(c)	I	0	0	0	103(24)	14.2(3)	14.0
Mn(2)	32(e)	II	2249(6)	2249(6)	2249(6)	498(74)	10.9(5)	10.0
Mn(3)	32(e)	I′	666(12)	666(12)	666(12)	232(145)	5.2(5)	4.0
Cs(1)	32(e)	II′	1637(4)	1637(4)	1637(4)	773(58)	7.3(2)	7.0
Cs(2)	32(e)	II	2642(3)	2642(3)	2642(3)	303(38)	7.6(2)	7.0
Cs(3)	48(f)	III	4245(2)	1250	1250	634(17)	21.8(3)	22.0

(b) $Mn_{21.5}Rb_{49}$-X

Atom	Wyc. Pos.	Site	*x*	*y*	*z*	U_{iso}[b]	Occupancy[c] Varied	Occupancy[c] Fixed
Si	96(g)		–540(3)	1225(5)	345(3)	133(16)		96
Al	96(g)		–544(4)	366(4)	1235(6)	251(20)		96
O(1)	96(g)		–1106(8)	10(11)	1047(7)	476(64)		96
O(2)	96(g)		–64(10)	–53(10)	1459(6)	417(54)		96
O(3)	96(g)		–337(6)	688(8)	643(8)	244(52)		96
O(4)	96(g)		–667(6)	844(6)	1718(7)	21(41)		96
Mn(1)	16(c)	I	0	0	0	204(40)	11.4(3)	11.5
Mn(2)	32(e)	II′	2054(11)	2054(11)	2054(11)	447(165)	5.9(6)	6.0
Mn(3)	32(e)	I′	609(14)	609(14)	609(14)	137(155)	3.9(5)	4.0
Rb(1)	32(e)	I′	963(12)	963(12)	963(12)	1217(252)	4.9(4)	5.0
Rb(2)	32(e)	II	2552(2)	2552(2)	2552(2)	357(24)	18.8(3)	18.0
Rb(3)	32(e)	II′	1687(10)	1687(10)	1687(10)	722(129)	6.4(4)	6.0
Rb(4)	48(f)	III	4145(5)	1250	1250	682(42)	21.4(5)	20.0

[a]Positional and thermal parameters are given $\times 10^4$. Numbers in parentheses are the esds in the units of the least significant digit given for the corresponding parameter. [b]$U_{iso} = (B_{iso}/8\pi^2)$. [c]Occupancy factors are given as the number of atoms or ions per unit cell.

height of 1.8 eÅ^{-3}. Simultaneous refinement of positional and isotropic thermal parameters for the framework atoms, Mn(1), Mn(2), Mn(3), Cs(1), Cs(2) and Cs(3) converged to $R_1 = 0.065$ and $R_2 = 0.049$.

Distinguishing Mn^{2+} from Cs^+ ions is easy for several reasons. First, their atomic scattering factors are very different (23 e^- for Mn^{2+} versus 54 e^- for Cs^+). Second, their ionic radii are different (Mn^{2+} = 0.80 Å versus Cs^+ = 1.69 Å). Also, the distances between Mn^{2+} ions and oxygens in the zeolite framework determined in dehydrated Mn_{46}-X[8] can be used as a criteria for distinction.

The occupancies of Mn(1), Mn(2), Mn(3), Cs(1), Cs(2), and Cs(3) were fixed at the values shown in Table 2(a), considering the cationic charge per unit cell. The final error indices converged to $R_1 = 0.069$ and $R_2 = 0.054$. The largest difference peak was found at (0.201, 0.201, 0.201). However, this peak was not refined as Mn^{2+} ions and was not considered further. The final refinement, the results of which are shown in Table 2(a), was done using the 385 reflections for which $I > 0$ to make better use of the diffraction data: $R_1 = 0.208$ and, $R_2 = 0.061$. This allowed the esds to decrease by about 40 % of the former values. Atomic scattering factors for $(Si, Al)^{1.75+}$, O^-, Mn^{2+}, and Cs^+ were used.[26,27] The function describing $(Si, Al)^{1.75+}$ is the mean of the Si^0, Si^{4+}, Al^0, and Al^{3+} functions. All scattering factors were modified to account for anomalous dispersion.[28] The final structural parameters and selected interatomic distances and angles are presented in Table 3(a).

$Mn_{21.5}Rb_{49}$-X. A full-matrix least-squares refinement was initiated, using the atomic parameters of the framework atoms in dehydrated Mn_{46}-X.[8] The isotropic refinement of the framework atoms converged to $R_1 = 0.41$ and $R_2 = 0.48$.

A difference Fourier function revealed three large peaks at (0.0, 0.0, 0.0), (0.246, 0.246, 0.246), and (0.415, 0.125, 0.125), with heights of 14.1, 12.6, and 6.6 eÅ^{-3}, respectively. These three peaks were stable in the least-square refinement. The isotropic refinement, including these peaks as Mn^{2+} ions at Mn(1) and Rb^+ ions at Rb(2) and Rb(4), converged to $R_1 = 0.147$ and $R_2 = 0.156$.

A subsequent difference Fourier synthesis revealed two additional peaks, at Rb(1) (0.080, 0.080, 0.080), with a height of 3.3 eÅ^{-3}, and at Mn(2) (0.204, 0.204, 0.204), with a height of 2.8 eÅ^{-3}. The isotropic refinement of framework atoms and these cations converged to $R_1 = 0.105$ and $R_2 =$

Table 3. Selected Interatomic Distances (Å) and Angles (deg)[a]

(a) $Mn_{28}Cs_{36}$-X

(Si, Al)-O(1)	1.66(1)	O(1)-(Si,Al)-O(2)	112.3(4)
(Si, Al)-O(2)	1.69(1)	O(1)- (Si, Al)-O(3)	104.5(4)
(Si, Al)-O(3)	1.66(1)	O(1)- (Si, Al)-O(4)	112.1(3)
(Si, Al)-O(4)	1.64(1)	O(2)- (Si, Al)-O(3)	110.8(5)
Mean (Si, Al)-O	1.66	O(2)- (Si, Al)-O(4)	105.6(6)
Mn(1)-O(3)	2.39(1)	O(3)- (Si, Al)-O(4)	112.4(3)
Mn(2)-O(2)	2.16(1)	(Si, Al)-O(1)- (Si, Al)	129.1(4)
Mn(3)-O(3)	2.53(1)	(Si, Al)-O(2)- (Si, Al)	134.9(7)
Cs(1)-O(2)	3.14(1)	(Si, Al)-O(3)- (Si, Al)	116.9(5)
Cs(2)-O(2)	2.93(1)	(Si, Al)-O(4)- (Si, Al)	115.6(4)
Cs(3)-O(4)	3.10(1)	O(3)-Mn(1)-O(3)	93.1(3)
		O(2)-Mn(2)-O(2)	117.9(4)
		O(3)-Mn(3)-O(3)	86.3(2)
		O(2)-Cs(1)-O(2)	72.2(3)
		O(2)-Cs(2)-O(2)	78.5(2)
		O(4)-Cs(3)-O(4)	59.1(2)

(b) $Mn_{21.5}Rb_{49}$-X

Si-O(1)	1.56(2)	O(1)-Si-O(2)	107.3(9)
Si-O(2)	1.68(2)	O(1)-Si-O(3)	110.9(9)
Si-O(3)	1.60(2)	O(1)-Si-O(4)	111.3(9)
Si-O(4)	1.56(2)	O(2)-Si-O(3)	110.1(9)
Mean Si-O	1.60	O(2)-Si-O(4)	109.1(9)
		O(3)-Si-O(4)	108.1(9)
Al-O(1)	1.71(2)	O(1)-Al-O(2)	110.2(9)
Al-O(2)	1.67(2)	O(1)-Al-O(3)	104.1(9)
Al-O(3)	1.75(2)	O(1)-Al-O(4)	108.8(9)
Al-O(4)	1.71(2)	O(2)-Al-O(3)	110.9(9)
Mean Al-O	1.71	O(2)-Al-O(4)	108.7(9)
		O(3)-Al-O(4)	109.1(9)
Mn(1)-O(3)	2.48(2)	Si-O(1)-Al	131.4(9)
Mn(2)-O(2)	2.30(3)	Si-O(2)-Al	139.2(9)
Mn(3)-O(3)	2.34(2)	Si-O(3)-Al	132.5(9)
Rb(1)-O(3)	3.37(2)	Si-O(4)-Al	158.2(9)
Rb(2)-O(2)	2.71(2)	O(3)-Mn(1)-O(3)	90.7(6)
Rb(3)-O(2)	3.09(2)	O(2)-Mn(2)-O(2)	113.6(8)
Rb(4)-O(4)	2.86(2)	O(3)-Mn(3)-O(3)	96.6(7)
		O(3)-Rb(1)-O(3)	62.5(6)
		O(2)-Rb(2)-O(2)	90.7(7)
		O(2)-Rb(3)-O(2)	76.6(5)
		O(4)-Rb(4)-O(4)	65.1(5)

[a]Numbers in parentheses are the estimated standard deviations in the units of the least significant digit given for the corresponding value.

0.083.

Based on successive difference Fourier functions, another two peaks were found, one at (0.170, 0.170, 0.170), with a height of 1.5 eÅ^{-3}, and another at (0.059, 0.059, 0.059), with a height of 1.3 eÅ^{-3}. The isotropic refinement that included these peaks as ions at Rb(3) and Mn(3) lowered the error indices to R_1 = 0.086 and R_2 = 0.069.

All shifts in the final cycle of least-squares refinement were less than 0.01% of their corresponding standard deviations. Considering the cationic charge per unit cell, the occupancies of Mn(1), Mn(2), Mn(3), Rb(1), Rb(2), Rb(3), and Rb(4) were fixed at the values shown in Table 2(b). The final error indices converged to R_1 = 0.087 and R_2 = 0.071. The largest difference peak was found at (0.348, 0.348, 0.348). However, this peak was too far from the framework oxygen and was not considered further. The final refinement, the results of which are shown in Table 2(b), was performed using the 682 reflections for which $I > 0$ to make more use of the diffraction data: R_1 = 0.296 and R_2 = 0.109. This allowed the esds to decrease by about 21% of the former values.

Atomic scattering factors for Si^0, Al^0, O^-, Rb^+, and Mn^{2+} were used.[26,27] The final structural parameters and selected interatomic distances and angles are presented in Table 3(b).

Discussion

Zeolite X is a synthetic version of the mineral faujasite, having opened, negatively charged frameworks (see Figure 1). Exchangeable cations, which balance the negative charge of the aluminosilicate framework, are found within the zeolites cavities. Cations are usually found at the sites as shown in Figure 1: site I at the center of the double six-ring (D6R), site I′ in the sodalite cavity on the opposite side of either of the D6Rs six-rings from site I, site II′ inside the sodalite cavity near a single six-ring (S6R), site II at the center of the S6R or displaced from this point into a supercage, site III on a 2-fold axis in the supercage opposite a four-ring between two 12-rings, and various III′ sites somewhat or a substantial distance from III but otherwise near the inner walls of the supercage or the edges of 12-rings.

$Mn_{28}Cs_{36}$-X. In this structure, 28 Mn^{2+} ions occupy three crystallographic sites and 36 Cs^+ ions occupy three different sites (see Table 2(a)). 14 Mn^{2+} ions at Mn(1) fill the octa-

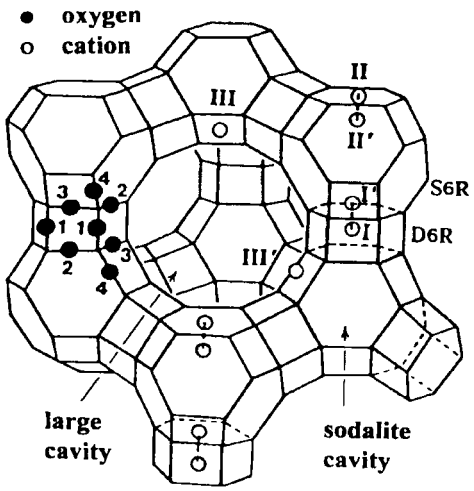

Figure 1. A stylized drawing of the framework structure of zeolite X. Near the center of the each line segment is an oxygen atom. The numbers 1 to 4 indicates the different oxygen atoms. Silicon and aluminum atoms alternate at the tetrahedral intersections. Si substitutes for about 4% of the Al's. Extraframework cation positions are labeled with Roman numerals.

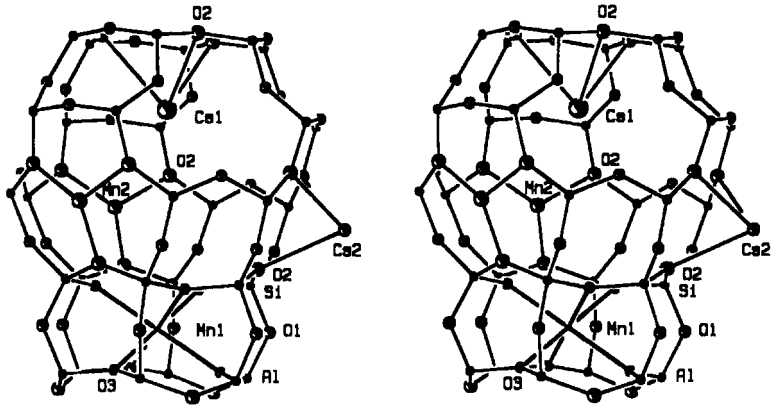

Figure 2. A stereoview of a sodalite cavity with an attached D6R in dehydrated $Mn_{28}Cs_{36}$-X. One Mn^{2+} ion at Mn(1) (site I), one Mn^{2+} ion at Mn(2) (site II), one Cs^+ ion at Cs(1) (site II′), and one Cs^+ ion at Cs(2) (site II) are shown. About 75% of sodalite cavities may have this arrangement. Ellipsoids of 20% probability are shown.

hedral site I (see Figure 2). The octahedral Mn(1)-O(3) distance of 2.39(1) Å is a little longer than the sum of the ionic radii of Mn^{2+} and O^{2-} (0.80 + 1.32 = 2.12 Å).[29] Because every site I is surrounded by two I′ sites, the neighboring positions, I and I′, cannot be occupied simultaneously due to the strong electrostatic repulsion between ions. Thus, the remaining four I′ sites are filled by Mn^{2+} ions at Mn(3). The bond distance of Mn(3)-O(3), 2.53(1) Å, is somewhat longer than the sum of the ionic radii of Mn^{2+} and O^{2-} (2.12 Å).[29] The remaining ten Mn^{2+} ions at Mn(2) are found at site II in the supercage (see Figures 2 and 3). Each Mn^{2+} ion at Mn(2) coordinates to three framework oxygens at 2.16(1) Å, which is almost the same as the sum of the corresponding ionic radii, and is recessed *ca*. 0.47(1) Å into the supercage from the plane of these three O(2)'s (see Table 4). The O(2)-Mn(2)-O(2) bond angle is 117.9(4)°, which is a nearly trigonal planar configuration. Mn^{2+} ions at Mn(2) form ionic bonds with three framework oxygens, O(3).

7 Cs^+ ions at Cs(1) are found at site II′ on a threefold axis in the sodalite cavity. Each Cs^+ ion lies relatively far inside the sodalite cavity, 2.14(1) Å, from the plane of the three O(2) framework oxygens. The bond distance of Cs(1)-O(2), 3.14(1) Å, is slightly longer than the sum of the corresponding ionic radii of Cs^+ and O^{2-} (1.69 + 1.32 = 3.01 Å).[29] 7 Cs^+ ions at Cs(2) are found at site II, on a threefold axis in the supercage. Each Cs^+ ion lies relatively far inside the supercage, 2.16(1) Å, from the plane of the three O(2) framework oxygens. The bond distance of Cs(2)-O(2), 2.93(1) Å, is almost the same as the sum of the corresponding ionic radii of Cs^+ and O^{2-} (3.01 Å).[29] Cs^+ ions at Cs(2) form ionic bonds with three O(2) framework oxygens. The remaining 22 Cs^+ ions occupy the 48-fold Cs(3) position at site III in the supercage. The Cs(3)-O(4) distance, 3.10(1) Å, is a little longer than the sum of the corresponding ionic radii of Cs^+ and O^{2-} (3.01 Å).[29] Plausible ionic arrangements for a sodalite cavity and a supercage are shown in Figures 2 and 3.

Table 4. Deviations (Å)[a] of Atoms and Cations from 6-ring Planes

	$Mn_{28}Cs_{36}$-X			$Mn_{21.5}Rb_{49}$-X		
	Cations	Site	Deviations (Å)	Cations	Site	Deviations (Å)
At O(3)[b]	Mn(1)	I	1.302	Mn(1)	I	1.420
	Mn(3)	I′	–2.35(2)	Mn(3)	I′	–1.19(2)
				Rb(1)	I′	–2.71(2)
At O(2)[c]	Mn(2)	II	0.47(1)	Rb(2)	II	1.876(4)
	Cs(2)	II	2.16(1)	Mn(2)	II′	–0.26(2)
	Cs(1)	II′	–2.14(1)	Rb(3)	II′	–1.83(1)

[a]Numbers in parentheses are the estimated standard deviations in the units of the least significant digit given for the corresponding parameter. [b]The positive and negative deviations indicate that the atom lies in a D6R and in the sodalite cavity, respectively. [c]The positive and negative deviations indicate that the atom lies in the supercage and in the sodalite cavity, respectively

In Mn_{46}-X,[8] 16 Mn^{2+} ions are at site I, and 30 Mn^{2+} ions are at site II. Mn^{2+} ions fill the site I positions. However, in $Mn_{28}Cs_{36}$-X, due to the successive Cs^+ ion exchanges, some of the Mn^{2+} ions at site II exchanged with Cs^+ ions, and were displaced from their initial positions. Mn^{2+} ions at site I are also affected by the exchanging Cs^+ ions. However, Cs^+ ions are too large to exchange with Mn^{2+} ions at site I. Thus, the Cs^+ ion exchange shows the cation-sieve effect. In this experiment, the maximum Cs^+ ion exchange was 39%. Mn^{2+} ions occupy sites I, I′, and II. The large Cs^+ ions occupy sites II, II′, and III.

$Mn_{21.5}Rb_{49}$-X. The mean values of Si-O and Al-O bond lengths are 1.60 Å and 1.71 Å, respectively. This justifies the ordering of Si and Al atoms in the lattice, and the choice of space group $Fd\bar{3}$ is proven. These mean values of the bond lengths are somewhat sensitive to ion exchanges and dehydration The individual Si-O and Al-O bond lengths show marked variations: Si-O from 1.56(2) Å to 1.68(2) Å, and Al-O from 1.67(2) Å to 1.75(2) Å. The occupancy of Mn^{2+} and Rb^+ ions in the same sodalite cavity induces the distortion of the framework structure (Si-O(2) = 1.68(2) Å and Al-O(2) = 1.67(2) Å) (see Table 3(b)) because strong electrostatic repulsion between cations has occurred,.

In this structure, 21.5 Mn^{2+} ions occupy three crystallographic sites, and 49 Rb^+ ions occupy four different sites. 11.5 Mn^{2+} ions at Mn(1) occupy the octahedral site I. The octahedral Mn(1)-O(3) distance of 2.48(2) Å is somewhat

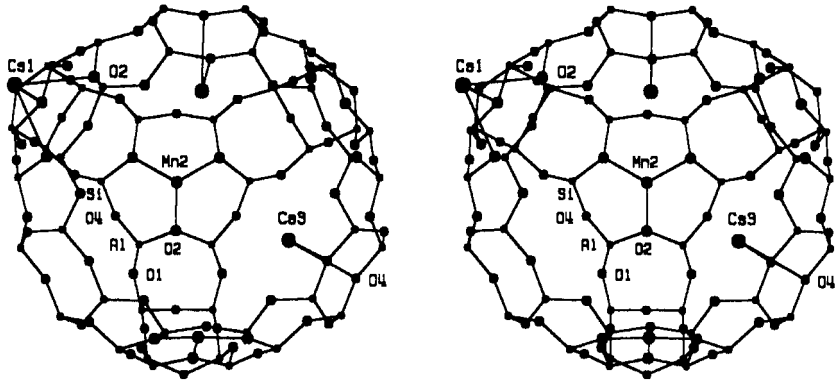

Figure 3. A stereoview of a supercage in dehydrated $Mn_{28}Cs_{36}$-X. One Mn^{2+} ion at Mn(2) (site II), one Cs^+ ion at Cs(1) (site II′), one Cs^+ ion at Cs(2) (site II), and three Cs^+ ions at Cs(3) (site III) are shown. About 50% of the supercages may have this arrangement. Ellipsoids of 20% probability are shown.

longer than the sum of the ionic radii of Mn^{2+} and O^{2-} (2.12 Å).[29] The remaining nine I′ sites are filled by 4 Mn^{2+} ions at Mn(3) and by 5 Rb^+ ions at Rb(1). Each Mn^{2+} ion at Mn(3) coordinates to three O(3) framework oxygens at 2.34(2) Å and is recessed *ca*. 1.19(2) Å into the sodalite cavity from the plane of these three O(2)s (see Table 4). These Mn-O bond distances are reasonable, considering the coordination numbers of Mn^{2+} ions. Mn^{2+} ions at Mn(1) and Mn(3) coordinate to six and three O(3) framework oxygens, respectively. 6 Mn^{2+} ions at Mn(2) are at site II′ in the sodalite cavity. Each Mn^{2+} ion coordinates to three O(2) framework oxygens at 2.30(3) Å and is recessed *ca*. 0.26(2) Å into the sodalite cavity from the plane of these three O(2)'s.

5 Rb^+ ions at Rb(1) and 6 Rb^+ ions at Rb(3) lie respectively at sites I′ and II′ on a threefold axis inside the sodalite cavity (see Figures 4 and 5). The Rb(1)-O(3) distance,

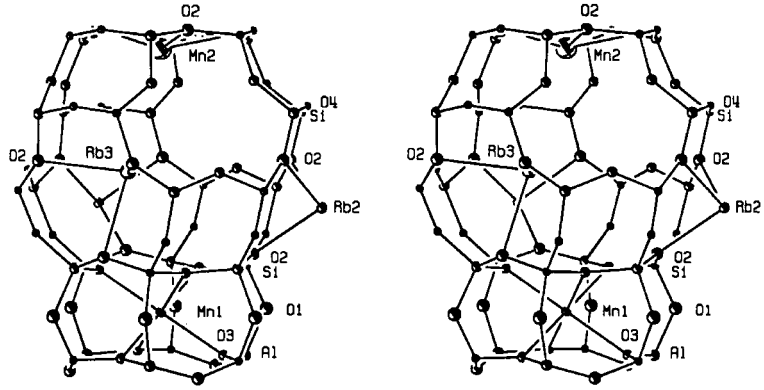

Figure 4. A stereoview of a sodalite cavity with an attached D6R in dehydrated $Mn_{21.5}Rb_{49}$-X. One Mn^{2+} ion at Mn(2) (site II′), one Rb^+ ion at Rb(1) (site I′), and two Rb^+ ions at Rb(2) (site II) are shown. About 50% of sodalite cavities may have this arrangement. Ellipsoids of 20% probability are shown.

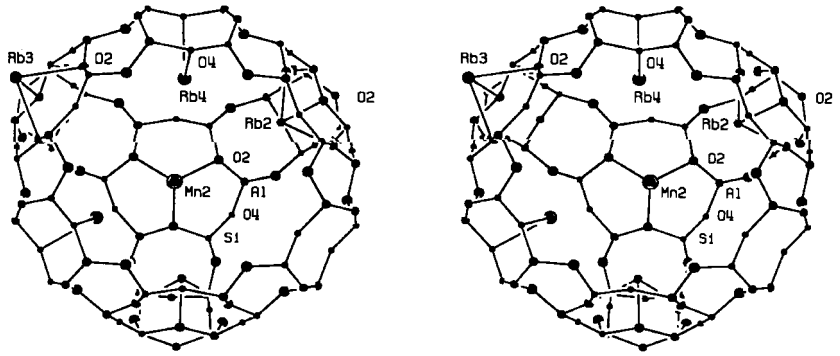

Figure 5. A stereoview of a supercage in dehydrated $Mn_{21.5}Rb_{49}$-X. One Mn^{2+} ion at Mn(2) (site II′), two Rb^+ ions at Rb(2) (site II), one Rb^+ ion at Rb(3) (site II′), and two Rb^+ ions at Rb(4) (site III) are shown. About 37.5% of supercages may have this arrangement. Ellipsoids of 20% probability are shown.

3.37(2) Å, is longer than the sum of the ionic radii of Rb^+ and O^{2-} (1.47 + 1.32 = 2.79 Å),[29] which indicate that these ions are loosely held to the framework oxygens. These ions lie relatively far inside the sodalite cavity, 2.71(2) Å, from the plane of these three O(3)'s. Each Rb^+ ion at Rb(3) coordinates to three O(2) framework oxygens at 3.09(2) Å and is recessed *ca*. 1.83(1) Å into the sodalite cavity from the plane of these three O(2)'s. 18 Rb^+ ions at Rb(2) are at site II in the supercage. The bond distance of Rb(2)-O(2), 2.71(2) Å, is almost the same as the sum of the ionic radii (2.79 Å).[29] Each Rb^+ ion at Rb(2) is recessed 1.876(4) Å into the supercage from the plane of the single six-ring. The remaining 20 Rb^+ ions occupy the 48-fold Rb(4) position at site III in the supercage. The Rb(4)-O(4) distance, 2.86(2) Å, is similar to the sum of the ionic radii of Rb^+ and O^{2-} (2.79 Å).[29] The plausible ionic arrangements for a sodalite unit and a supercage are shown in Figures 4 and 5, respectively.

The site selectivity for $Mn_{21.5}Rb_{49}$-X can be explained by considering the relative ionic size and charge of Mn^{2+} and Rb^+ ions. The Na^+ ions in zeolite X can be fully exchanged with the small and highly charged Mn^{2+} ions.[8] In Mn_{46}-X, Mn^{2+} ions occupy sites I and II. Some Mn^{2+} ions at site II are exchanged with Rb^+ ions and are displaced from their initial positions by the successive Rb^+ ion exchange. Rb^+ ions occupy sites II, II′, and III. Mn^{2+} ions at site I are also affected by the exchanging Rb^+ ions. Some of the Mn^{2+} ions at site I are displaced from their initial positions and are exchanged with the Rb^+ ions, but the Rb^+ ions are too large to lie in the double-six rings. The Rb^+ ion exchange shows the cation-sieve effect. In this experiment, the maximum Rb^+ ion exchange was 53%.

In Na-X, the Cs^+ and Rb^+ ion exchange could be achieved to 65-80%.[17-19] However, in the structures of $Mn_{28}Cs_{36}$-X and $Mn_{21.5}Rb_{49}$-X, the maximum degree of Cs^+ and Rb^+ ion exchange was only 39% and 53%, respectively. The Mn^{2+} ions at site I are more strongly held by six O(3) framework oxygens than the Na^+ ions at site I. The cation-sieve effects of zeolites toward the Cs^+ and Rb^+ ions can be attributed to the following mechanisms: (1) Cs^+ and Rb^+ ions are too large to enter the small cavities, (2) the charge distribution on the zeolite structure may be unfavorable, and (3) the sizes of hydrated cations in the aqueous solution may influence the exchange of cations.

The ion exchange in zeolites is controlled by diffusion of ions within the crystal structure. The diffusion rate of the Rb^+ ion in chabazite at 25 °C[30] is *ca*. 40 times faster than that of the Cs^+ ion. The relative ionic diameters of Rb^+ and Cs^+ ions are 2.94 Å and 3.38 Å.[29] Therefore, the Cs^+ and the Rb^+ ion exchange in Mn_{46}-X can be summarized as follows: the relatively smaller Rb^+ ions can diffuse faster through the small hexagonal window of 2.2 Å in free diameter than Cs^+ ions can. Therefore, Rb^+ ions can occupy sites I′ and II′ in the sodalite cavity, whereas Cs^+ ions only occupy site II′ in the sodalite cavity. This may be attributed to the degree of Cs^+ and Rb^+ ion exchange in Mn^{2+}-exchanged zeolite X, to be restricted to 39% and 53%, respectively. When these large Cs^+ and Rb^+ ions occupy sites II′ and I′, they lie far inside the sodalite cavity. About 1.4 Mn^{2+} or Cs^+ cations and 2.6 Mn^{2+} or Rb^+ cations are present in every sodalite cavity of $Mn_{28}Cs_{36}$-X and $Mn_{21.5}Rb_{49}$-X, respectively. The repulsion between cations in the same sodalite cavity induces the distortion of the structure.

Acknowledgment. This work was supported in part by the Korea Research Foundation made in the program year of 2000 (Grant No. 2000-15-DP0190).

References

1. Breck, D.W. *Zeolite Molecular Sieves*; Wiley Jones: New York, 1974.
2. Treacy, M. M. J.; Mercus, B. K.; Bisher, M. E.; Higgins, J. B. *Proceedings of the 12th International Zeolite Conference*; Materials Research Society: Pennsylvania, 1999; Vol. I-IV.
3. Olson, D. H. *Zeolites* **1995**, *15*, 439.
4. Vitale, G.; Mellot, C. F.; Bull, L. M.; Cheetham, A. K. *J. Phys. Chem. B* **1997**, *101*, 4559.
5. Porche, F.; Souhassou, M.; Dusausoy, Y.; Lecomte, C. *Eur. J. Mineral*. **1999**, *11*, 333
6. Zhu, L.; Seff, K. *J. Phys. Chem. B* **1999**, *103*, 9512.
7. Yeom, Y. H.; Jang, S. B.; Kim, Y.; Song, S. H.; Seff, K. *J. Phys. Chem. B* **1997**, *101*, 6914.
8. Jang, S. B.; Jeong, M. S.; Kim, Y.; Seff, K. *J. Phys. Chem. B* **1997**, *101*, 9041.
9. Kim, M. J.; Jeong, M. S.; Kim, Y.; Seff, K. *Micro. Meso. Mat.* **1999**, *30*, 233.
10. Bae, D.; Seff, K. *Micro. Meso. Mat.* **1999**, *33*, 265.
11. Lee, S. H.; Kim, Y.; Seff. K. *J. Phys. Chem. B* **2000**, *104*, 2490.
12. Lee, S. H.; Kim, Y.; Seff. K. *J. Phys. Chem. B* **2000**, *104*, 11162.
13. Lee, S. H.; Kim, Y.; Seff. K. *Micro. Meso. Mat.* **2000**, *41*, 49.
14. Yoon, B. Y.; Song, M. K.; Lee, S. H.; Kim, Y. *Bull. Korean Chem. Soc*. **2001**, *22*, 30.
15. Song, M. K.; Yoon, B. Y.; Kim, Y. *Bull. Korean Chem. Soc*. **2001**, *22*, 164.
16. Mortier, W. J. *Compilation of Extra-framework Sites in Zeolites*; Butterworth Scientific Ltd.: Guildford, U.K., 1982.
17. Barrer, R. M.; Rees, L. V. C.; Shamsuzzoha, M. *J. Inorg. Nucl. Chem*. **1966**, *28*, 629.
18. Barrer, R. M.; Meier, W. M. *Trans. Faraday Soc*. **1959**, *55*, 130.
19. Theng, B. K. G.;Vansant, E.; Uytterhoeven, J. B. *Trans. Faraday Soc*. **1968**, *64*, 3370.
20. Jang, S. B.; Song, S. H.; Kim. Y. *J. Korean Chem. Soc*. **1996**, *40*, 427.
21. Jang, S. B.; Jeong, M. S.; Han, Y. W.; Kim, Y. *Bull. Korean Chem. Soc*. **1996**, *17*, 631.
22. Bogomolov, V. N.; Petranovskii, V. P. *Zeolites* **1986**, *6*, 418.
23. *Structure Determination Package Programs, MolEN*; Enraf-Nonius: Netherlands, 1990.
24. *International Tables for X-ray Crystallography*; Kynoch Press: Birmingham, England, 1974; Vol. II, p 302.
25. Zhu, L.; Seff, K.; Olson, D. H.; Cohen, B. J.; Von Dreele, R. B. *J. Phys. Chem. B* **1999**, *103*, 10365.

26. *International Tables for X-ray Crystallography*; Kynoch Press: Birmingham: England, 1974; Vol IV, pp 73-87.
27. Cromer, D. T. *Acta Crystallogr.* **1965**, *18*, 17.
28. *International Tables for X-ray Crystallography*; Kynoch Press: Birmingham, England, 1974; Vol IV, pp 149-150.
29. *Handbook of Chemisty and Physics*, 70th ed.; The Chemical Rubber Co.: Cleveland, Ohio, 1989/1990; pp. F-187.
30. Barrer, R. M.; Bartholomew, R.; Rees, L. V. C. *J. Phys. Chem. Solids* **1963**, *24*, 51.